J Mater Sci (2007) 42:3343–3348
DOI 10.1007/s10853-006-0744-x

SIZE-DEPENDENT EFFECTS

EPR analysis of the local structure of Ni^{3+} ions in Ni-based electrode materials obtained under high-pressure

Ekaterina Zhecheva · Radostina Stoyanova · Elitza Shinova

Received: 22 May 2006 / Accepted: 31 July 2006 / Published online: 26 April 2007

Abstract X-band and high-frequency EPR spectroscopy was applied to monitor the short-range cation ordering in Ga, Al and Li substituted $LiNiO_2$ with a layered crystal structure. The mixed oxides were obtained by a high-pressure synthesis in an oxygen rich atmosphere. Analysis of the EPR line-width from the X-band experiments together with the values of the g-tensor from the high-frequency EPR experiments permits assesing the local structure of the mixed metal layers. The results obtained show that $LiGa_yNi_{1-y}O_2$, $LiAl_yNi_{1-y}O_2$ and $Li_{1+x}Ni_{1-x}O_2$ are homogeneous solid solutions, whereas the $Li_{1+x}Ni_{1-x-y}Al_yO_2$ compositions have rather a complex domain structure of the type *(1–a)*$LiAl_yNi_{1-y}O_2$.*a*$Li[Li_{1/3}Ni_{2/3}]O_2$.

Introduction

Lithium nickelates, $LiNiO_2$, with layered crystal structure have been considered as potential electrode materials for lithium ion batteries due to their lower cost and environmental benignity [1–4]. The electrochemical reaction is based on the reversible oxidation/reduction of the Ni^{3+}/Ni^{4+} ions in the NiO_2-layers which takes place in the course of electrochemical lithium deintercalation/intercalation from the LiO_2-layers. Despite the fact that enormous research and technological efforts have been devoted to improving the electrochemical performance of cathode materials, the cycling stability is still unsatisfactory. One approach to improve the cycling stability of layered $LiNiO_2$ is to replace Ni^{3+} by electrochemically inactive metal ions [1–4]. The role of these metal dopants is to enhance the thermal stability of oxides in delithiated state, to limit the depth of lithium intercalation/deintercalation, and to increase the potential of electrochemical Li extraction.

With a view to improvement of the electrochemical performance of $LiNiO_2$-based materials, more detailed study of the relationship between the local effect in solids and their intercalation properties is to be carried out. In this respect, spectroscopic methods such as solid state nuclear magnetic resonance [5], Raman scattering and Fourier transform-infrared spectroscopy [6], as well as Mössbauer techniques [7], permit more precise examination of the local cationic structure in solids.

Electron paramagnetic resonance (EPR) spectroscopy deals not only with the electronic structure of paramagnetic centres, but also with their local environments. This assertion is referred to paramagnetic ions both in magnetically diluted and concentrated systems. The aim of this contribution is to summarize the results obtained by EPR spectroscopy as a local probe technique for analysis of nickel-based electrode materials doped with Al, Ga and Li. In order to achieve maximal solubility of Al, Ga and Li in the metal layer, for the preparation of Al, Ga and Li-substituted $LiNiO_2$ and of Li substituted $LiAl_yNi_{1-y}O_2$ we have used a high-pressure synthesis in an oxygen rich atmosphere.

Experimental

The preparation of Ga, Al and Li substituted $LiNiO_2$ and of Li substituted $LiAl_yNi_{1-y}O_2$ under high-

E. Zhecheva (✉) · R. Stoyanova · E. Shinova
Institute of General and Inorganic Chemistry, Bulgarian Academy of Sciences, 1113 Sofia, Bulgaria
e-mail: zhecheva@svr.igic.bas.bg

pressure in an oxygen rich atmosphere is described elsewhere [8–10]. Under high pressure, solid Li $[Ga_yNi_{1-y}]O_2$ solutions with a layered crystal structure can be obtained in the whole concentration range: $0 \le y \le 1$ [8]. The formation of layered solid solutions between $LiNiO_2$ and α-$LiAlO_2$, $LiAl_yNi_{1-y}O_2$, proceeds for $0 \le y < 0.5$ and $0.8 < y \le 1$. In addition, high-pressure synthesis in an oxygen-rich atmosphere yields novel layered compositions with an enhanced Li-to-metal ratio: $Li[Li_xNi_{1-x}]O_2$ with $0 \le x \le 1/3$, and $Li[Li_xAl_yNi_{1-x-y}]O_2$ with $y < (1-y)/3$ and $y = 0.05$ and 0.10 [9, 10]. The crystal structure of $Li[Li_{1/3}Ni_{2/3}]O_2$ is changed from trigonal *R*-3m to monoclinic *C*2/m at a Li-to-Ni ratio of 2 (or $x = 1/3$).

X-ray phase analysis was carried out on a Philips X'Pert powder diffractometer, with CoKα1, reflection mode, and with a Si internal standard. The scan range $15 \le 2\Theta \le 120$ in a step increment of 0.02° was utilized. The computer program Fullprof was used for the calculation. The diffractometer point zero, Lorentzian/Gaussian fraction of the pseudo-Voigt peak function, scale factor, lattice constants (*a* and *c*), oxygen parameter (*z*), thermal factors for 3*a*, 3*b* and 6*c* positions, halfwidth parameters, preferred orientation were refined. To gain stability during the refinement, the Ga/Al/Li-to-Ni-ratio was imposed by the chemical composition. Subsequently, the cationic occupancy factors were refined taking into account that the total occupancies of the 3*a* and 3*b* sites were equal to unity.

Electron Paramagnetic Resonance (EPR) measurements at 9.23 GHz (X-band) were carried out a ERS 220/Q spectrometer within the temperature range 85–410 K. The g-factors were established with respect to a Mn^{2+}/ZnS standard. The high-frequency EPR spectra were recorded on a single-pass transmission EPR spectrometer built in the High-Magnetic Filed Laboratory, Grenoble, France. The frequencies were changed from 95 to 345 GHz using Gunn diodes and their multipliers. The detection of absorption was performed with a bolometer. The recording temperatures were varied from 5 to 300 K using a variable temperature insert (Oxford Instruments).

Results and discussions

Crystal chemistry of Ga, Al and Li substituted $LiNiO_2$

A structural feature of $Li[Ga/Al_yNi_{1-y}]O_2$ and $Li[Li_xNi_{1-x}]O_2$ compositions as compared to the well-known $Li[Ni]O_2$ is the development of mixed $[Ga/Al_yNi_{1-y}]O_2$ and $[Li_xNi_{1-x}]O_2$-layers in addition to nearly pure Li-layers [8–10]. For $Li[Li_xNi_{1-x}]O_2$, the replacement of Ni^{3+} by Li^+ is compensated for by the appearance of Ni^{4+} ions [9].

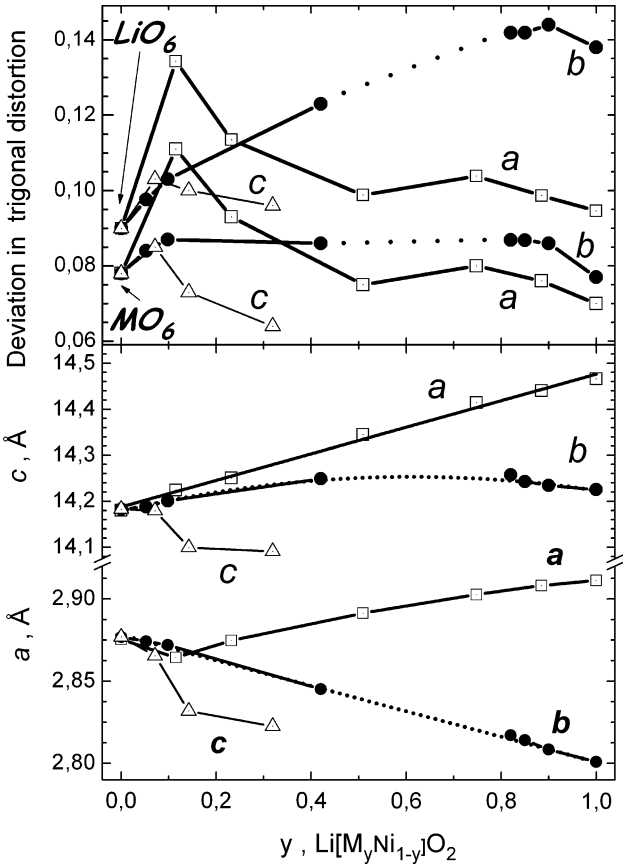

Fig. 1 Changes in the unit cell parameters *a* and *c* and deviation of the experimentally determined extent of the trigonal distortion of the LiO_6- and $M_yNi_{1-y}O_6$-octahedra from that of the undistorted octahedron.for Ga (a), Al (b) and Li (c) substituted $LiNiO_2$

The evolution of the unit cell dimensions (*a* and *c*) with the Al, Ga and Li substitution is shown in Fig. 1. (For the sake of comparison, the end composition $Li[Li_{1/3}Ni_{2/3}]O_2$ is also indexed in *R*-3m.) The unit cell parameter *a* (which expresses the metal–metal distance in the layer) decreases with the Al content, while Ga dopants lead to an expansion of *a*. The observed dependence is in accordance with the ionic dimensions of Al^{3+}, Ga^{3+} and Ni^{3+} ions. The *c*-parameter increases monotonously with the Ga content, but for Al-substituted oxides *c* increases sharper with the Al content as compared to a linear interpolation of the *c* parameter calculated from the two end members $LiNiO_2$ and $LiAlO_2$. In the case of Li substituted $LiNiO_2$, there is a strong contraction in both *a* and *c* parameters due to the appearance of Ni^{4+} ions. The observed variation in the unit cell parameters *a* and *c* reveals the structural anisotropy of the layered structure. The ratio between

the distance separating two opposite faces of the octahedron and the *a*-parameter can be used as a measure of the mean trigonal distortion of the MO_6-octahedra. Figure 1 shows the deviation of the experimentally determined extent of the trigonal distortion of the LiO_6- and $M_yNi_{1-y}O_6$-octahedra from that of the undistorted octahedron. (For an undistorted octahedron this ratio is 0.816). It is noticeable that the LiO_6-octahedra are more flexible to tolerate the increased trigonal distortion as compared to the $M_yNi_{1-y}O_6$-octahedra (Fig. 1). While the mean trigonal distortion of LiO_6-, $Ga_yNi_{1-y}O_6$- and $Li_xNi_{1-x}O_6$-octahedra changes simultaneously with the Ga and Li content, respectively, for Al-substituted oxides there is strong increase in the extent of the trigonal distortion for LiO_6–octahedral as compared to that of the $Al_yNi_{1-y}O_6$ octahedra.

EPR spectroscopy of Ga and Al substituted $LiNiO_2$, $LiGa/Al_yNi_{1-y}O_2$

Nearly stoichiometric $LiNiO_2$ has been shown to exhibit an EPR spectrum consisting of a single Lorentzian line with $g = 2.137$ due to low spin Ni^{3+} ions [11]. The line shape and line width depend on the registration temperature due to the Jahn-Teller effect and ferromagnetic interactions between Ni^{3+} ions in the layers [11, 12]. In the EPR spectra of Al- and Ga-substituted oxides, a Lorentzian line is still visible except for $LiAlO_2$ and $LiGaO_2$ doped with 1% Ni (Fig. 2). Figure 3 compares the dependence of the EPR line width on the Ni^{3+}-content for both series. As one can see, the EPR line width increases with the Al and Ga content, passing through a maximum at about 50 %, and decreasing with further increase of the Al and Ga contents. These changes in the EPR line width are typical of magnetically concentrated systems, where both dipole-dipole and exchange interactions take place [13–15]. Depending on the spin concentration and the distance between the spins, the dipole-dipole interactions are superimposed on the Zeeman's interactions, thus leading to an increase in line width. Contrary to the dipole-dipole interactions, the exchange interactions average the local magnetic fields around the paramagnetic species, as a result of which the line width decreases [13–15]. The competition between dipole-dipole and exchange interactions determines the dependence of the EPR line width on the concentration of Ni^{3+} ions. The effect of Ga on the EPR line width of Ni^{3+} is most pronounced as compared to that of Al.

The temperature variation of the EPR line width, ΔH_{pp}, is also affected by the Al and Ga substitution

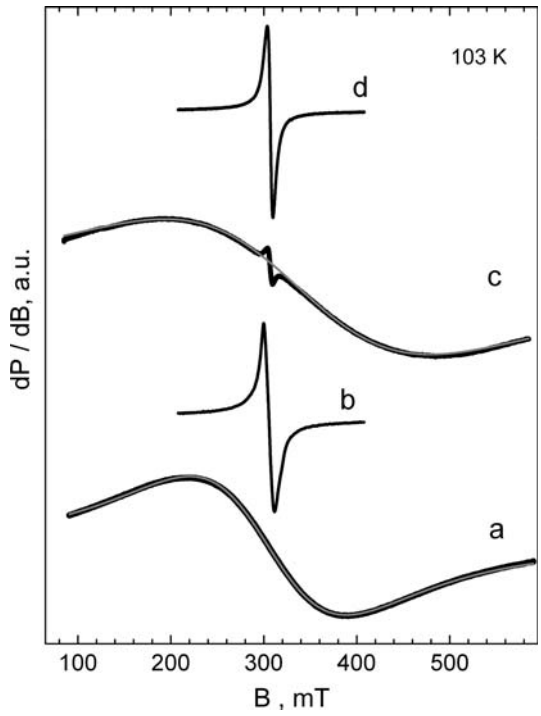

Fig. 2 X-band EPR spectra at 103 K of Li $Al_{0.25}Ni_{0.75}O_2$ (**a**), Li $Al_{0.9}Ni_{0.1}O_2$ (**b**), $LiGa_{0.25}Ni_{0.75}O_2$ (**c**) and $LiGa_{0.9}Ni_{0.1}O_2$ (**d**)

(Fig. 4). For oxides with $0 \le y \le 0.25$, there is a linear decrease in the EPR line width on cooling, while for oxides with $y \ge 0.5$ the EPR line width slightly depends on the registration temperature. For pure $LiNiO_2$, the $d\Delta H_{pp}/dT$ slope has been shown to depend on the strength of the 180°- and 90°-$Ni^{3+/2+}$-O-$Ni^{3+/2+}$ exchange interactions, the metal coordination number of the exchange-coupled particles and on the distance between them [12]. The slope of the linear

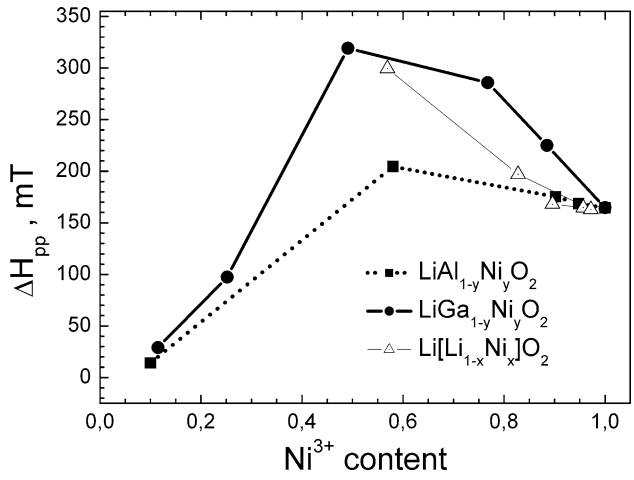

Fig. 3 Changes of the EPR line width (ΔH_{pp}) at 103 K with the Ni^{3+} content of Al, Ga and Li substituted $LiNiO_2$

dependence, $d\Delta H_{pp}/dT$, decreases with the reduction of the amount of Ni^{2+} in the lithium layers [12]. Further decrease in $d\Delta H_{pp}/dT$ is observed when Al (or Ga) substitutes for Ni, $Li_{1-\delta}Ni_{\delta}[Al/Ga_yNi_{1-y}]O_2$ (Fig. 4). This result also demonstrates the formation of solid solutions between $LiAlO_2$ and $LiNiO_2$.

Contrary to Al-substituted oxides, a narrow signal with a lower intensity and $g = 2.14$ superimposed on the main Lorentzian line can be resolved in the EPR spectrum of Ga-substituted oxides, irrespective of the Ga content (Fig. 2). The line width of the narrow signal does not depend on the Ga-content. High-frequency EPR spectroscopy (HF EPR) allows more clearly differentiation between both signals. Thus, the cationic distribution in $LiGa_{0.1}Ni_{0.9}O_2$ has been studied by HF-EPR at 115 GHz (Fig. 5). At 5 K, two signals are observed in the EPR spectra recorded at 115 GHz: one Lorentzian signal with $g = 2.140 \pm 0.001$ and one tetragonally asymmetric signal with $g_{\perp} = 2.191$ and $g_{\parallel} = 2.041$. The line width for the broad Lorentzian decreases with heating: $\Delta H_{pp} = 111 \pm 5$ mT at 5 K, 70 ± 4 mT at 30 K and 56.9 ± 1.9 mT at 60 K. In addition, the Lorentzian signal detected at 115 GHz can be compared with the broad Lorentzian detected in the X-band EPR spectrum of $LiGa_{0.1}Ni_{0.9}O_2$: $\Delta H_{pp} = 29.0 \pm 1.1$ mT at 103 K. The increased line width can be related to complex enveloping resulting from the convolution of the lines due to the magnetic dipole-dipole and exchange coupled Ni^{3+}. On heating, the tetragonal signal displays a tendency to coalesce into one symmetrical line, which can be resolved in the X-band EPR spectrum as a narrow Lorentzian. According to the EPR study of Ni^{3+} in $LiNi_xCo_{1-x}O_2$ solid solutions [16], these two EPR signals can be assigned to Ni^{3+} ions having different paramagnetic/diamagnetic metal environments. Thus, the broad signal corresponds to Ni^{3+} ion having mixed Ni/Ga environment, while the tetragonally asymmetric signal is due, most probably, to Ni^{3+} in diamagnetic environment (pure Ga). For the sake of comparison, Fig. 5 shows also theEPR spectrum of Ni^{3+} spin probes in the diamagnetic matrix of $LiGa_{0.1}Co_{0.9}O_2$.

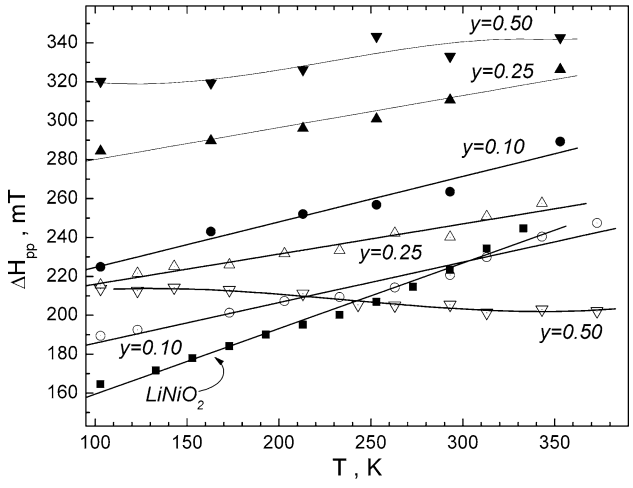

Fig. 4 Temperature variation of the EPR line width (ΔH_{pp}) of nearly stoichiometric $LiNiO_2$, $LiAl_yNi_{1-y}O_2$ (open symbols) and $LiGa_yNi_{1-y}O_2$ (full symbols)

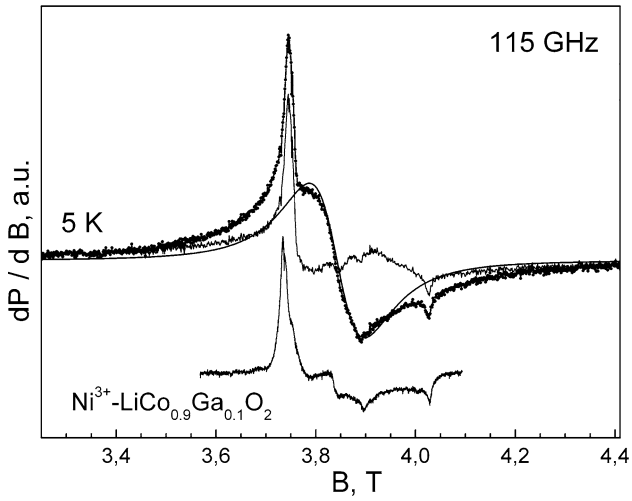

Fig. 5 High-frequency EPR spectra at 5 K of $LiGa_{0.9}Ni_{0.1}O_2$ and of Ni^{3+} spin probes in the diamagnetic matrix of $LiGa_{0.1}Co_{0.9}O_2$

EPR spectroscopy of Li substituted $LiNiO_2$ and $LiAl_yNi_{1-y}O_2$, $Li_{1+x}Ni_{1-x}O_2$ and $Li_{1+x}Al_yNi_{1-x-y}O_2$

A broad signal with the g value of 2.13 is observed for $Li[Li_xNi_{1-x}]O_2$ oxides. The EPR line width increases and the intensity of the EPR signal decreases with the amount of lithium incorporated in the nickel layer (Fig. 6). For the end composition $Li[Li_{1/3}Ni_{2/3}]O_2$, the broad signal disappears and a narrow low-intensity signal with g = 2.14 appears instead. According to the EPR study of Ni^{3+} in $LiNi_xCo_{1-x}O_2$ solid solutions [16], the parameters of the two EPR signal of $Li[Li_xNi_{1-x}]O_2$ suggest that the broad signal may be attributed to exchange-coupled Ni^{3+} ions, while the narrow low-intensity signal comes from magnetically isolated Ni^{3+} ions. The increase in line width with the amount of lithium in the $Li_xNi_{1-x}O_2$-layers can be explained as a result of magnetic dilution of the paramagnetic Ni^{3+} ions by the diamagnetic Ni^{4+} ions which appear for charge compensation. The smooth decrease in the EPR line width of $Li[Li_xNi_{1-x}]O_2$ with the Li content indicates the formation of solid solutions between $LiNiO_2$

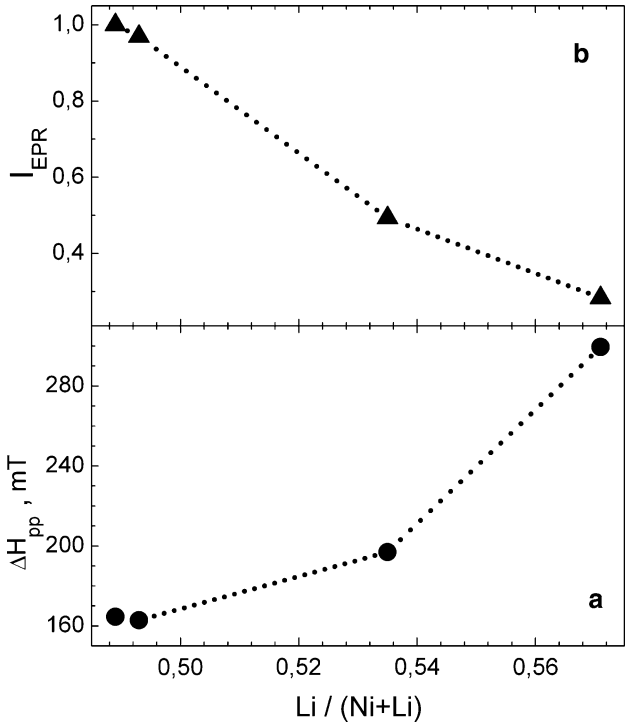

Fig. 6 Changes in the EPR line width (ΔH_{pp}) and in the EPR signal intensity (I_{EPR}) with the lithium content in $Li_{1+x}Ni_{1-x}O_2$

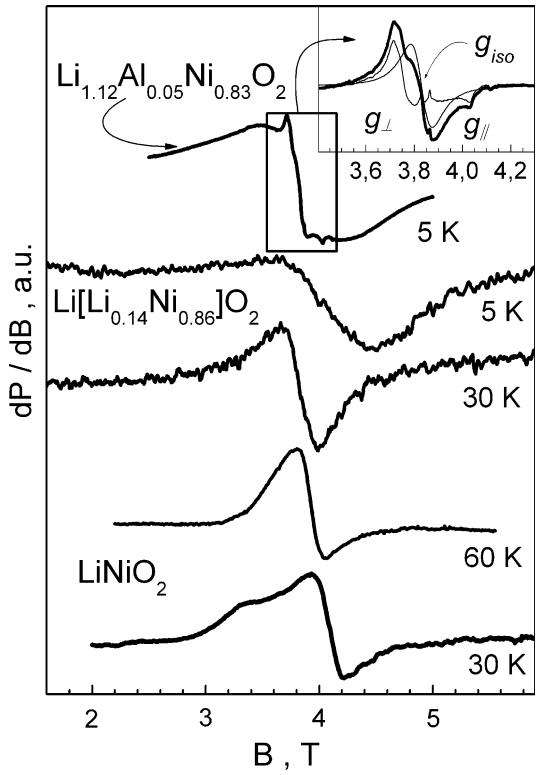

Fig. 7 High-frequency EPR spectra of $LiNiO_2$, $Li_{1.14}Ni_{0.86}O_2$ and $Li_{1.12}Al_{0.05}Ni_{0.83}O_2$

and $Li[Li_{1/3}Ni_{2/3}]O_2$. For the end composition $Li[Li_{1/3}Ni_{2/3}]O_2$, the EPR signal comes from isolated Ni^{3+} ions only, whose surroundings include diamagnetic ions (Li^+ and/or Ni^{4+} ions).

Additional differentiation between the samples containing lithium in the nickel layers can be achieved by EPR spectroscopy at high frequencies (HF-EPR) due to the better resolution as compared to conventional X-band EPR [17]. Figure 7 shows the EPR spectra at 115 GHz of nearly stoichiometric $LiNiO_2$ and $Li[Li_xNi_{1-x}]O_2$ samples obtained from precursors with Li:Ni ratios of 1.2 and 1.5, respectively. Above 30 K the EPR spectrum of paramagnetic $Li_{1-\delta}Ni_{1+\delta}O_2$ consists of an asymmetric line. Below 30 K the appearance of resonance absorption in high- and low field indicates the presence of magnetically correlated spins (Fig. 7). However, long-range magnetic ordering is not achieved with this sample. In contrast to $LiNiO_2$, $Li[Li_xNi_{1-x}]O_2$ containing Li in the nickel layers displays only one broad symmetric Lorentzian line above 13 K even in the high-frequency region (Fig. 7). The line width decreases with increasing temperature from 13 to 80 K, the g-value remaining constant: 2.155. In this temperature range the signal intensity varies with the registration temperature following the Curie-Weiss law with a Weiss constant $\Theta_{EPR} = +4$ K. The Weiss constant thus determined is lower than the Weiss constant determined for $LiNiO_2$ prepared from a precursor with Li/Ni = 1.2: $\Theta_{EPR} = +43$ K, X-band. At temperatures below 13 K the EPR line shape for $Li[Li_xNi_{1-x}]O_2$ undergoes a change, most possibly due to short-range magnetic correlations. Similarly to the case of $LiNiO_2$, a long-range magnetic ordering down to 5 K cannot be achieved with the $Li[Li_xNi_{1-x}]O_2$ sample. This result shows clearly that the EPR spectrum of $Li[Li_xNi_{1-x}]O_2$ is due to low-spin Ni^{3+} ions. However, in contrast to nearly stoichiometric $LiNiO_2$, the low-spin Ni^{3+} ions in $Li[Li_xNi_{1-x}]O_2$ are magnetically diluted. The lack of any additional EPR signals in high-frequency EPR spectrum also supports that $Li_{1-\delta}Ni_{\delta}[Li_xNi_{1-x}]O_2$ represents a solid solution.

For Li substituted $LiAl_yNi_{1-y}O_2$ ($Li_{1+x}Al_yNi_{1-x-y}O_2$ with $x = 0.12$ and $y = 0.05$), the high-frequency EPR spectrum at 5 K displays three overlapping signals (Fig. 7). The appearance of these latter signals can be associated with Ni^{3+} ions having different local environment in respect to paramagnetic Ni^{3+} and diamagnetic $Al^{3+}/Ni^{4+}/Li^+$ ions. The main signal is with an asymmetric shape and line width of about 1.4 T. This EPR signal has parameters corresponding to those of Ni^{3+} in a Ni^{3+}-rich environment. The other two signals have a low intensity as compared to the

main broad signal. One of them is a single Lorentzian line with $g = 2.144$ and a line width of 89 mT which can be assigned to Ni^{3+} ions having mainly diamagnetic neighbors and only small amount of paramagnetic Ni^{3+} ions. The second low-intensity signal has a line with an axial symmetry: $g_{\|} = 2.038$ and $g_{\perp} = 2.196$. The axially symmetric line indicates that this signal comes from Ni^{3+} with only diamagnetic ions as first neighbors. Moreover, for $Li_{1+x}Al_yNi_{1-x-y}O_2$, the observed values of the g-tensor indicate that the magnetically isolated Ni^{3+} ions are surrounded by diamagnetic Ni^{4+} rather than by Al^{3+}.

The detection of tree types of Ni^{3+} ions $Li_{1+x}Al_yNi_{1-x-y}O_2$ reveals compositional inhomogeneities in the mixed Ni, Li, AlO_2-layers and demonstrates the appearance of domains in the layered structure having different amount of Ni^{3+} ions. Thus, from HF-EPR experiments one may assume that the $Li_{1+x}Al_yNi_{1-x-y}O_2$ compositions have a complex domain structure of the type *(1-a)*$LiAl_yNi_{1-y}O_2$.*a*$Li[Li_{1/3}Ni_{2/3}]O_2$ rather than homogeneous solid solutions. Formation of a local domain structure has also been established by NMR and TEM analysis for the complex ''$LiNi/MnO_2$–Li_2TiO_3'' system [18, 19].

Conclusions

We have demonstrated that the combination of X-band and high-frequency EPR spectroscopy is an effective tool to assess the short-range cation distribution in Ga, Al and Li substituted $LiNiO_2$. Layered $LiGaNi_{1-y}O_2$, $LiAl_yNiO_2$ and $Li_{1+x}Ni_{1-x}O_2$ are homogeneous solid solutions whereas the $Li_{1+x}Al_yNi_{1-x-y}O_2$ compositions have rather a complex domain structure of the type *(1-a)*$LiAl_yNi_{1-y}O_2$.*a*$Li[Li_{1/3}Ni_{2/3}]O_2$

Acknowledgements The authors thank the National Science Fund of Bulgaria (Contract no. Ch1304/2003) for financial support. R.S. and E.Sh. are grateful to the EC for a grant of a EU ''Research Infrastructures: Transnational Access'' Programme (Contract No. 505320 (RITA) – High Pressure) for performing high-pressure synthesis experiments at the Bayrisches Geoinstitute. The high-frequency EPR measurements carried out at High Magnetic Field Laboraty in Grenoble, France, were supported by the European Commission within the 6th framework programme ''Transnational Access - Specific Support Action'' (contract No. RITA-CT-2003-505474) – ''Access to research in very high magnetic field''. The authors are very grateful to Dr. T. Boffa-Ballaran and Dr. C. McCammon, from Bayerisches Geoinstitut, Universität Bayreuth, and Dr. A.-L. Barra, from High Magnetic Field Laboratory in Grenoble, for their help.

References

1. Brousesely M, Biensan P, Simon B (1999) Electrochim Acta 45:3
2. Delmas C, Menetrier M, Croguennec L, Saadoune I, Rougier A, Poillerie C, Prado G, Grüne M, Fournes L (1999) Electrochim Acta 145:243
3. Alcántara R, Lavela P, Tirado J-L, Zhecheva E, Stoyanova R (1999) J Solid State Electrochem 3:121
4. Whittingham MS (2004) Chem Rev 104:4271
5. Grey CP, Dupre N (2004) Chem Rev 104:4493
6. Julien CM, Massot M, Poinsignon C (2004) Spectrochim Acta A 60:689
7. Alcántara R, Lavela P, Pérez-Vicente C, Tirado JL, Jumas JC, Olivier-Fourcade J (2000) Solid State Commun 115:115
8. Stoyanova R, Zhecheva E, Alcántara R, Tirado JL, Bromiley G, Bromiley F, Boffa Ballaran T (2004) J Mater Chem 14:363
9. Shinova E, Zhecheva E, Stoyanova R, Bromiley G (2005) J Solid State Chem 178:1661
10. Shinova E, Zhecheva E, Stoyanova R, Bromiley GD, Alcántara R, Tirado JL (2005) J Solid State Chem 178:2692
11. Stoyanova R, Zhecheva E, Friebel C (1993) J Phys Chem Solids 54:9
12. Stoyanova R, Zhecheva E, Friebel C (1994) Solid State Ionics 73:1
13. Van Vleck JH (1948) Phys Rev 74:1168
14. Anderson PW, Weiss PR (1953) Rev Mod Phys 25:269
15. Morya T (1956) Prog Theor Phys Kyoto 16:23
16. Stoyanova R, Zhecheva E, Alcántara R, Lavela P, Tirado JL (1997) Solid State Commun 102:457
17. Anderson KK, Barra AL (2002) Spectrochim Acta A 58:1101
18. Kim J-S, Johnson CS, Vaughey JT, Thackeray MM, Hackney SA, Yoon W, Grey CP (2004) Chem Mater 16:1996
19. Yoon W-S, Iannopollo S, Grey CP, Carlier D, Gorman J, Reed J, Ceder G (2004) Electrochem Solid-State Lett 7:A167